Article:
Carrilero, L., Dunn, S.J., Moran, R.A. et al. (2023) Evolutionary responses to acquiring a multidrug resistance plasmid are dominated by metabolic functions across diverse Escherichia coli lineages. mSystems, 8 (1). e0071322. ISSN: 2379-5077

https://doi.org/10.1128/msystems.00713-22

AMERICAN SOCIETY FOR MICROBIOLOGY | mSystems®

RESEARCH ARTICLE

Evolutionary Responses to Acquiring a Multidrug Resistance Plasmid Are Dominated by Metabolic Functions across Diverse *Escherichia coli* Lineages

Laura Carrilero,[a,b] Steven J. Dunn,[c] Robert A. Moran,[c] Alan McNally,[c] Michael A. Brockhurst[a]

[a]Division of Evolution, Infection and Genomics, School of Biological Sciences, University of Manchester, Manchester, United Kingdom
[b]School of Biosciences, University of Sheffield, United Kingdom
[c]Institute of Microbiology and Infection, College of Medical and Dental Science, University of Birmingham, Birmingham, United Kingdom

Laura Carrilero and Steven J. Dunn contributed equally to the article. Author order was determined alphabetically.

ABSTRACT Multidrug resistance (MDR) plasmids drive the spread of antibiotic resistance between bacterial lineages. The immediate impact of MDR plasmid acquisition on fitness and cellular processes varies among bacterial lineages, but how the evolutionary processes enabling the genomic integration of MDR plasmids vary is less well understood, particularly in clinical pathogens. Using diverse *Escherichia coli* lineages experimentally evolved for ~700 generations, we show that the evolutionary response to gaining the MDR plasmid pLL35 was dominated by chromosomal mutations affecting metabolic and regulatory functions, with both strain-specific and shared mutational targets. The expression of several of these functions, such as anaerobic metabolism, is known to be altered upon acquisition of pLL35. Interactions with resident mobile genetic elements, notably several IS-elements, potentiated parallel mutations, including insertions upstream of *hns* that were associated with its upregulation and the downregulation of the plasmid-encoded extended-spectrum beta-lactamase gene. Plasmid parallel mutations targeted conjugation-related genes, whose expression was also commonly downregulated in evolved clones. Beyond their role in horizontal gene transfer, plasmids can be an important selective force shaping the evolution of bacterial chromosomes and core cellular functions.

IMPORTANCE Plasmids drive the spread of antimicrobial resistance genes between bacterial genomes. However, the evolutionary processes allowing plasmids to be assimilated by diverse bacterial genomes are poorly understood, especially in clinical pathogens. Using experimental evolution with diverse *E. coli* lineages and a clinical multidrug resistance plasmid, we show that although plasmids drove unique evolutionary paths per lineage, there was a surprising degree of convergence in the functions targeted by mutations across lineages, dominated by metabolic functions. Remarkably, these same metabolic functions show higher evolutionary rates in MDR-lineages in nature and in some cases, like anaerobic metabolism, their expression is directly manipulated by the plasmid. Interactions with other mobile elements resident in the genomes accelerated adaptation by disrupting genes and regulatory sequences that they inserted into. Beyond their role in horizontal gene transfer, plasmids are an important selective force driving the evolution of bacterial genomes and core cellular functions.

KEYWORDS ESBL, *Escherichia coli*, ST131, antimicrobial resistance, cefotaxime, experimental evolution, horizontal gene transfer, plasmid

Escherichia coli is a common cause of human and animal infections. In particular, multidrug resistant (MDR) lineages cause serious invasive diseases and pose significant challenges for effective treatment (1). The emergence of these MDR lineages is typically

Editor Alejandra Rodríguez-Verdugo, University of California, Irvine

Address correspondence to Michael A. Brockhurst, michael.brockhurst@manchester.ac.uk.

The authors declare no conflict of interest.

Received 29 July 2022
Accepted 2 January 2023
Published 1 February 2023

associated with the acquisition of one or more multidrug resistance plasmids (2). Such plasmids often encode resistances against multiple antibiotic classes, including clinically important frontline treatments (3). In particular, the acquisition and dissemination of extended spectrum beta-lactamase (ESBL) genes in *E. coli* is largely mediated by the transfer of MDR plasmids (2). The ESBL gene $bla_{\text{CTX-M-15}}$ confers resistance to cephalosporins and has been widely disseminated by IS*Ecp1*, which contributes to mobilization of this gene between DNA molecules and increases its expression by replacing its native promoter (4). The abundance and diversity of ESBL plasmids in *E. coli* makes controlling their spread incredibly challenging. Understanding the factors that determine the successful integration of these plasmids into bacterial genomes is therefore a high priority.

The response of bacterial cells to plasmid acquisition can vary extensively between bacterial lineages. For example, multiple studies report that the immediate growth or fitness impact of acquiring an identical plasmid ranges from negative to positive between different lineages of a species (5–7). These differences have been linked to gene content variation among the bacterial genomes in some cases (5). In addition, the transcriptional response to plasmid acquisition can also vary between bacterial lineages in terms of the identity of differentially expressed chromosomal genes, the numbers of bacterial genes affected, and the magnitude of their change in expression level (6). Collectively, these comparative experimental data suggest that there will be lineage-specific or perhaps even genotype-specific responses to MDR plasmid acquisition that are contingent upon genetic variation among the recipient bacterial genomes.

In lineages where plasmid acquisition imposes high fitness costs and/or causes appreciable disruption to cellular function(s), we would expect plasmid carriage to be rare because plasmid-bearing cells will be selected against in antibiotic-free environments, where the benefits of plasmid encoded traits do not outweigh the fitness cost of plasmid carriage (8–11). However, an emerging theme in evolutionary studies of plasmid-host interactions is that plasmid acquisition often acts as a catalyst for evolutionary changes in the bacterial chromosome and/or the plasmid itself, which enable the stable genomic integration of newly acquired plasmid replicon(s) even when these are at first costly (12). Such evolutionary responses to plasmid acquisition can take the form of compensatory mutation(s) that resolve specific genetic conflicts between plasmid and chromosomal genes to ameliorate the cellular disruption these cause (13–16). Alternatively, these evolutionary responses can be more extensive, involving coadaptation of the chromosome and plasmid, whereby multiple mutations occurring on both replicons are necessary to assimilate the plasmid into the genome (17–19). To date, few studies have compared the evolutionary responses of diverse lineages to acquiring a new plasmid at the genomic level (16, 19, 20). As such little is known about how the evolutionary processes of genomic integration of an MDR plasmid vary between genomically diverse bacterial lineages.

Here we take a comparative experimental evolution approach to test how the evolutionary response to acquisition of the MDR plasmid pLL35 varies between genomically diverse lineages of *E. coli*. pLL35 is a 106 kb FII(K)-9 plasmid that was obtained from a *Klebsiella* clinical isolate (6). This plasmid replicon type is common among *Enterobacteriaceae,* including both *E. coli* and *Klebsiella* (21, 22). pLL35 has a complete, uninterrupted F-like transfer region and carries multiple antibiotic resistance genes, including $bla_{\text{CTX-M-15}}$, which confers resistance to cefotaxime (6). Replicate populations of five *E. coli* strains, including both environmental and clinical isolates and the lab strain MG1655, carrying pLL35 were serially passaged with or without cefotaxime for ~700 bacterial generations, alongside plasmid-free controls propagated without cefotaxime (respectively, these different treatments were named EX, EP, and EC). Bacterial population density and plasmid frequency was monitored over time by selective plating and colony PCR. At the end of the experiment, we compared the growth and cefotaxime resistance of evolved clones and obtained their whole-genome sequences and, for MG1655, the ancestral and evolved transcriptomes and conjugation rates. The growth response to selection varied between lineages and according to cefotaxime treatment, but no change in cefotaxime resistance was observed between treatments. We observed parallel

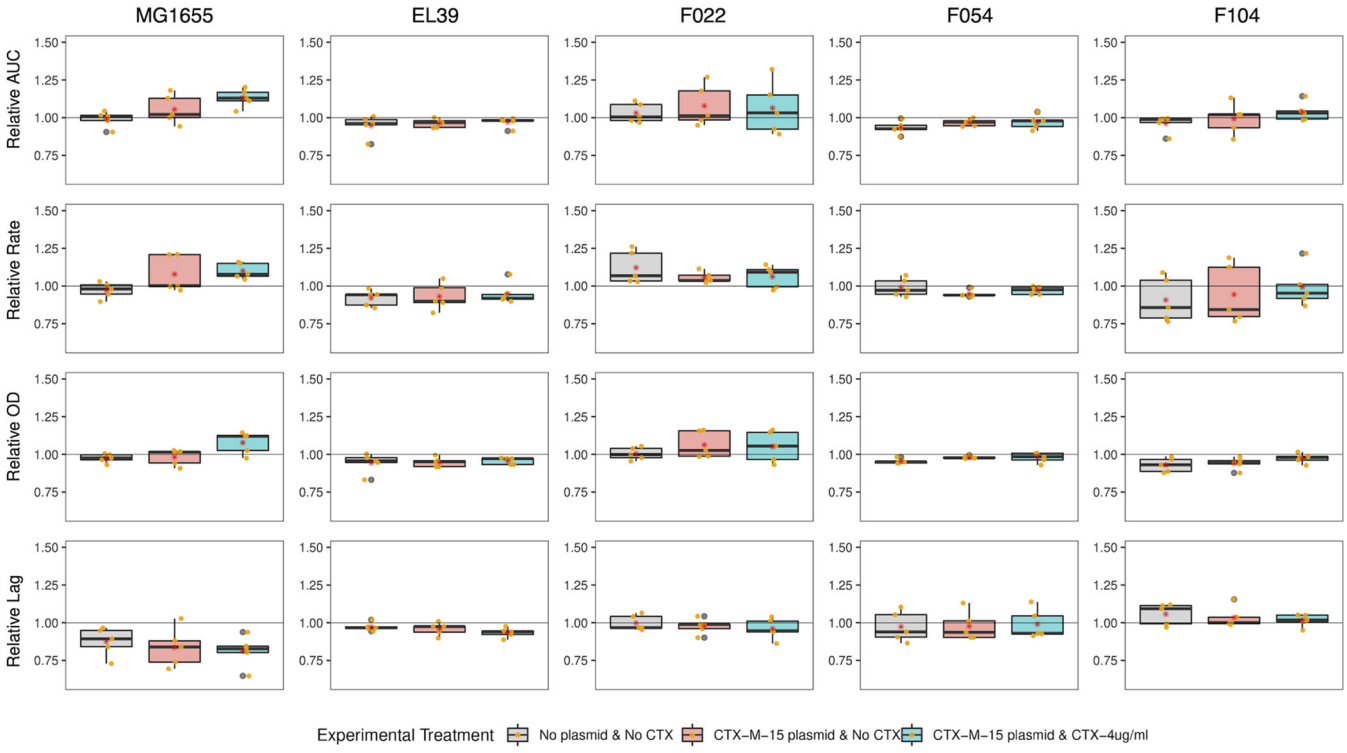

FIG 1 Growth kinetic parameters of evolved bacterial clones relative to their ancestor. Boxplots represent the change in growth kinetic parameters for evolved clones relative to their ancestor (i.e., for plasmid-free evolved clones this would be the relevant plasmid-free ancestral strain, whereas for plasmid-carrying evolved clones this would be the relevant plasmid-containing ancestral strain). Each strain is shown in a separate row and each growth kinetic parameter is shown in a different column, as indicated by the labels. Each evolution treatment is denoted by a color (gray, plasmid-free control, C; red, plasmid-carrier without cefotaxime, EP; blue, plasmid-carrier with cefotaxime, EX). Datapoints show the mean of technical replicates for each individual evolved clone.

mutations in evolved plasmid-carriers at loci or within operons associated with a range of functions, including cellular metabolism, regulation of MGEs, and plasmid conjugation.

RESULTS

Growth kinetic and resistance responses to selection. To test for the initial effect of plasmid acquisition on bacterial growth we compared growth kinetic parameters for each of the ancestral *E. coli* strains with or without pLL35. Acquisition of pLL35 reduced growth in the ancestral *E. coli* strains (Fig. S1; statistical tables provided in Table S1), indicating that plasmid carriage imposed a fitness cost in all strain genetic backgrounds used here. Despite this initial fitness cost of the plasmid, however, we observed no appreciable plasmid loss in any of the plasmid-containing populations during the ~700 generations selection experiment either with or without cefotaxime (Fig. S2), indicating that pLL35 was stably maintained regardless of positive selection for the encoded CTX-M-15 extended-spectrum beta-lactamase. Apart from MG1655 and ELU39, which were plasmid-free before the addition of pLL35, all evolved strains contained one or more coresident plasmids. At least one coresident plasmid in each strain was F-type (containing an FII or FIB replicon). Generally, coresident plasmids were maintained throughout the pLL35 evolution experiment, apart from the loss of the 122,292 bp FIB plasmid from F022 in three replicates (F022 EPB, F022 EPE, F022 EXA).

We next quantified the change in growth kinetic parameters and cefotaxime resistance for a randomly chosen evolved clone per replicate population from the end of the selection experiment relative to their ancestor (these evolved clones were also used in subsequent genome sequencing). The response of growth kinetic parameters to selection varied among strains and between treatments (Fig. 1; Table S1; raw data provided in Data Set S1). Notably, the strains MG1655 and F022 showed higher growth rates and maximum densities relative to their ancestors than did strains EL39, F104, and F054. Moreover, plasmid

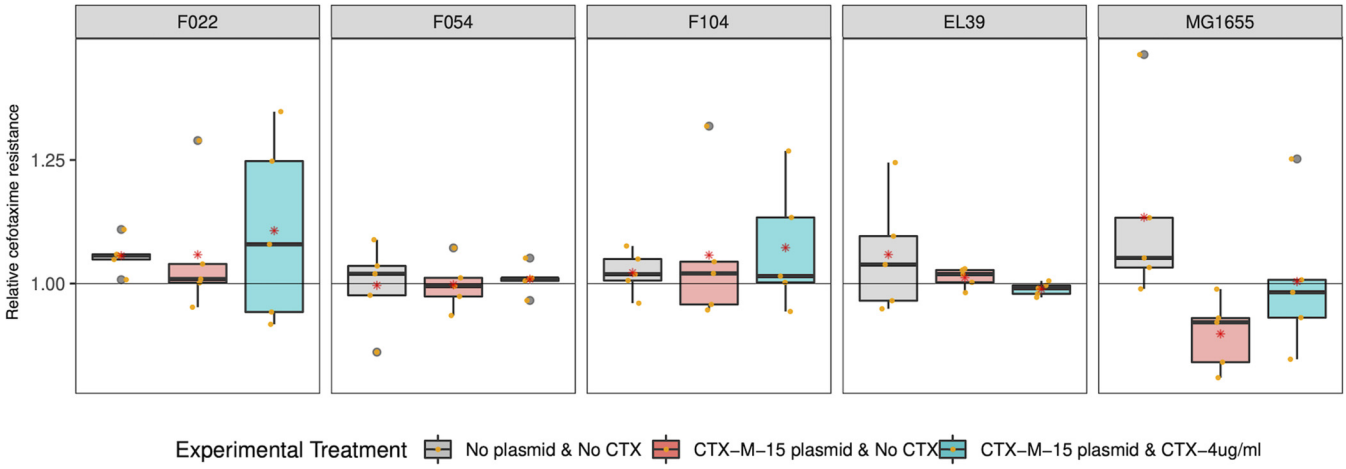

FIG 2 Cefotaxime resistance of evolved bacterial clones relative to their ancestor Boxplots represent the change in cefotaxime resistance following evolution as area under the MIC curve for evolved clones relative to their ancestor. Each strain is shown in a separate panel as indicated by the label. Each evolution treatment is denoted by a color (gray, plasmid-free control, C; red, plasmid-carrier without cefotaxime, EP; blue, plasmid-carrier with cefotaxime, EX). Datapoints show the mean of technical replicates for each individual evolved clone.

bearing clones evolved with cefotaxime tended to show higher performance across a range of growth kinetic parameters than evolved plasmid-free control clones. However, the relative level of resistance to cefotaxime in evolved plasmid carriers did not vary with strain or cefotaxime selection (ART ANOVA strain $F_{4,60} = 1.4161$ $P = 0.24$; cefotaxime selection $F_{2,60} = 2.8666$ $P = 0.06$; Fig. 2; Table S1; raw data provided in Data Set S1).

Genetic responses to selection. To determine the genetic response to selection and how this varied among strains and treatments we obtained whole-genome sequences for a randomly chosen evolved clone per replicate population (named A to E). Evolved clones had gained between 0 and 45 mutations, including mutations located both in the chromosome (range = 4 to 43 mutations) and the plasmid (range = 0 to 21 mutations) in the evolved plasmid-carrying clones. Four out of 50 evolved plasmid-carrying clones were hypermutators, having acquired mutations in mismatch repair, while none of the evolved clones from control populations were hypermutators. Excluding hypermutator clones, of all the observed SNVs, 12.1% ($n = 23$) were synonymous, 22.2% ($n = 42$) were intergenic, and the remaining 65.6% ($n = 124$) were nonsynonymous. The total, mean and median number of mutations across each treatment and replicate are provided in Table S2. There were also 18 instances of IS movement and 4 deletions. The number of nonsynonymous mutations per evolved clone did not vary among *E. coli* strains ($P = 0.0931$ ANOVA) or between treatments ($P = 0.6603$ ANOVA). Next, to distinguish mutations putatively associated with an evolved response to plasmid acquisition, we identified the subset of chromosomal loci acquiring mutations that were exclusive to plasmid-carriers (i.e., loci that never acquired mutations in the corresponding plasmid-free controls) for further analysis (Fig. 3). This subset contained 14 loci that were mutated in more than one independently evolved clone. Such parallel evolution is suggestive of selection having acted upon the mutations at these loci, which were then analyzed further. Functional analysis of these loci revealed enrichment for transcriptional regulators (*rpoS*, *putA*, *norR*, *nhaR*, *fadR*) and inorganic ion transport and metabolism (*putP*, *mgtA*, *artP*, *nanT*), with the remaining loci representing singleton COG categories.

At a number of chromosomal loci and operons we observed parallel evolution occurring between strains (~22% of SNVs, $n = 78$; Fig. 3, S3), suggesting a common evolved response to the plasmid among the divergent *E. coli* genetic backgrounds. The most commonly mutated locus was the arginine transporter gene *artP*, with mutations affecting 9 evolved clones across multiple replicates of F022 and ELU39 both with and without cefotaxime selection, and a single replicate of F054. Several of these mutations were clustered within a similar region of the ArtP protein, which encodes the main ABC transporter domain and may therefore affect arginine transport. Other transporters affected by mutations in multiple strains were the sialic acid transporter gene *nanT* and magnesium transporting

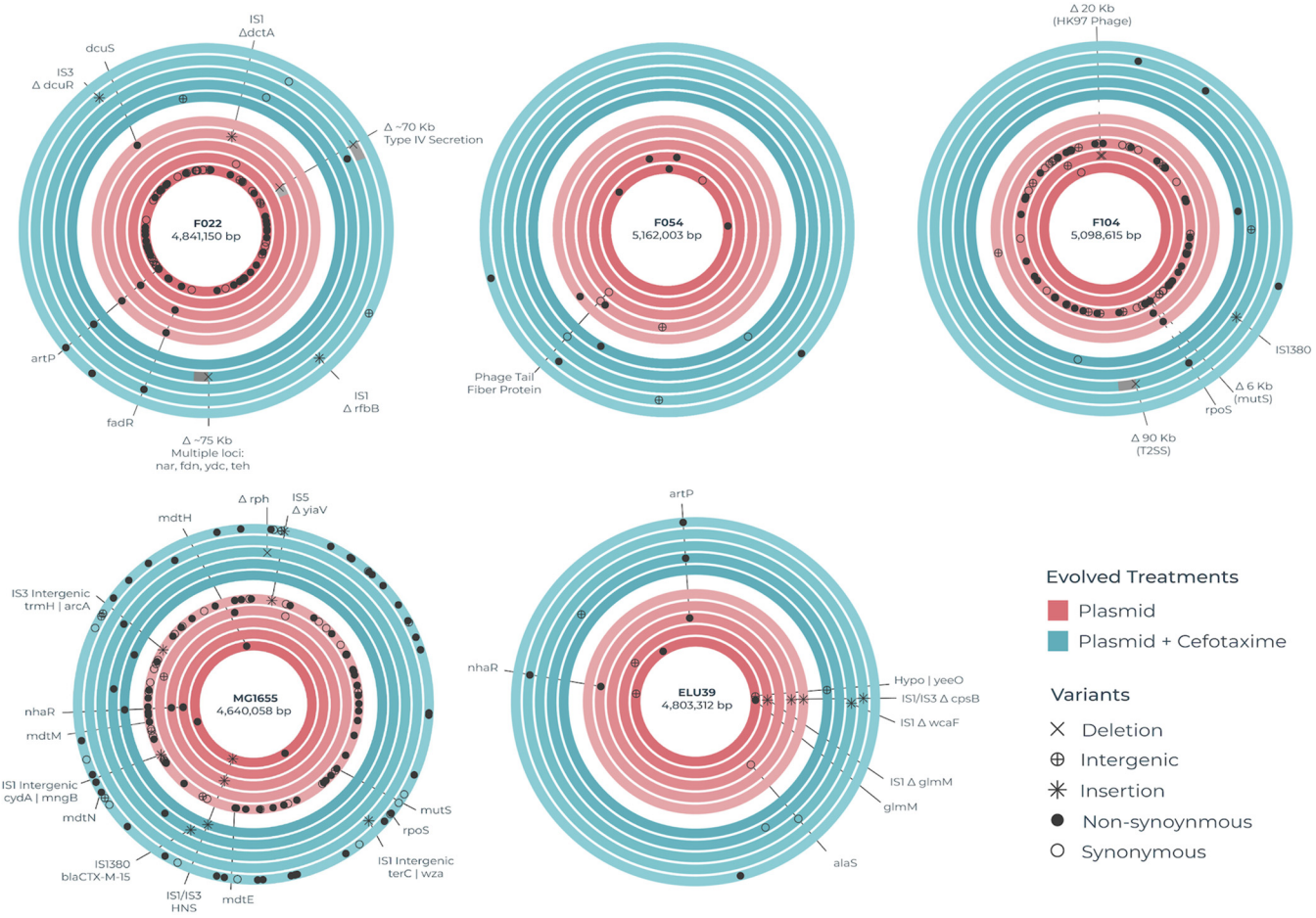

FIG 3 Chromosomal loci targeted by mutations in evolved plasmid-carriers. Each circular track represents the chromosome of an independently evolved clone, the replicates being sorted from A (inner) to E (outer). A single randomly chosen clone was genome sequenced per evolving line. As such the five replicate evolved clones per strain (as labeled) per treatment (Blue for plasmid-carriers evolved with cefotaxime, EX; Red for plasmid-carriers evolved without cefotaxime, EP) are shown as concentric tracks. Loci that acquired mutations during evolution in plasmid-carriers but not in the corresponding plasmid-free control are shown by markers denoting the type of mutation (see visual key). Loci that acquired parallel mutations in multiple independently evolving lines per strain per treatment have been labeled with the corresponding gene name or locus tag.

ATPase gene *mgtA*. Several other metabolic functions also displayed between strain parallelism. These included key components of anaerobic metabolism, including fatty acid metabolism and anaerobic respiration: *fadR,* a multifunctional regulator of fatty acid metabolism, was mutated in 4 evolved clones of strains ELU39 and F104 where mutations clustered between amino acid residues 29 to 35. In both cases, these residues occur in the turn between an alpha helix and beta strand of a putative HTH *gntR* type conserved domain, which may therefore have some transcriptional impact. In F104 a variant was detected in *fadI* from the same operon that catalyzes the final step in fatty acid oxidation. Mutations were observed in *norR* (A418A, A448V), an anaerobic nitric oxide reductase transcriptional regulator, in both MG1655 and F022. The sodium/proline metabolism *put* operon also exhibited between strain parallelism, with *putP* containing an identical D55G mutation across two replicates of F022, and a single MG1655 isolate. In the F022 isolates, *putA* gained mutations at two separate amino acid residues (L213P, Y1073H). Other functions displaying between strain parallelism included the transcriptional regulator *nhaR* controlling expression of the NhaA Na+/H+ antiporter protein in strains MG1655 and ELU39; the stress response sigma factor *rpoS* in strains MG1655 and F104; the mismatch repair gene *mutS* resulting in hypermutability in 4 evolved plasmid-carrying clones of strains MG1655, F104, and F022; and the glycerol metabolism operon *glp*.

In contrast, at several other loci we observed parallel evolution occurring only within evolved lines from a single strain, suggesting certain strain specific evolutionary

responses to plasmid acquisition. In MG1655 several genes in the multidrug resistance operon *mdt* contained nonsynonymous mutations, though no change in resistance to cefotaxime was detected in the clones carrying these mutations. Mutations were also observed in multiple MG1655 replicates in the *ydh* operon, including the monooxygenase *ydhR,* which is involved in the metabolism of aromatic compounds, as well as ABC transporter *yjj*. Other examples of within strain parallelism affected hypothetical genes without known functions. Of the ~78% of SNVs occurring as singletons among replicates, the majority related to transcriptional control or metabolic functions.

We observed multiple insertion sequence mediated mutations in evolved clones, suggesting that this was an important mutational mode for some strains in our study, although the propensity for IS-mediated mutations varied substantially among the *E. coli* strains. Whereas multiple IS-mediated mutations were observed in evolved clones of MG1655 (n = 8), F022 (n = 3), and ELU39 (n = 5), only a single IS-mediated mutation occurred in F104, and none were observed in F054. In three MG1655 evolved plasmid-carrying clones both with and without cefotaxime selection, we observed a common insertion of two separate insertion sequences (IS*1* & IS*3*) upstream of *hns* and thymidine kinase gene *tdk*, all within a 33 bp window (IS*1* EPC = 2,587,180, IS*1* EXA = 2,587,192, IS*3* EPA = 2,587,213). The 26 amino acids adjacent to *hns* were unaffected, suggesting that the *hns* promoter is likely intact, but the IS may form a discretely transcribed unit. In F104 and MG1655 we observed movement of an IS*Ecp1* transposition unit (TPU), originating from pLL35 and encompassing all or part of the adjacent $bla_{\text{CTX-M-15}}$ gene. In MG1655 a TPU that included the entire $bla_{\text{CTX-M-15}}$ inserted into the chromosome, but in F104 the smaller TPU only included a truncated $bla_{\text{CTX-M-15}}$. The duplication of $bla_{\text{CTX-M-15}}$ in MG1655 does not appear to have altered the cefotaxime MIC of the evolved clone. In ELU39 we observed a common truncation of mannose-1-phosphate guanylyltransferase gene *cpsB*, mediated by two different IS elements, and an IS-element insertion affecting the phosphoglucosamine mutase protein GlmM that does not interrupt the protein, but rather occupies the sequence immediately adjacent. Across two different replicates of ELU39, we observed an insertion of IS*3* in the two-component regulatory element *dcuR*, and a nonsynonymous mutation in the second component of that system, *dcuS*. This two component regulator controls anaerobic fumarate metabolism, and also weakly regulates the fumarate transporter encoded by *dctA*, in which we observed an insertion of IS*1* causing truncation of this gene. This suggests multiple routes likely to alter fumarate uptake and metabolism, and alongside mutations targeting other aspects of anaerobic metabolism across multiple strains (e.g., fatty acid metabolism and anaerobic respiration) indicates that anaerobic metabolism was a key target of selection in plasmid-carriers.

Few mutations were observed in the pLL35 plasmid sequence in the evolved clones (Table S2), with observed variants frequently targeting genes involved in plasmid conjugation (Fig. S4). Two evolved clones of F054 contained pLL35 with nonsynonymous mutations affecting *traD* encoding the coupling protein and *traI* encoding the multifunctional conjugation protein, and an evolved clone of MG1655 contained pLL35 with a nonsynonymous mutation affecting *traI*. In F104 an evolved clone from the cefotaxime selected treatment contained pLL35 with a complete deletion of the conjugational machinery that rendered the plasmid conjugation deficient. Excluding this deletion mutant, all other evolved plasmid-carrying clones retained the ability to conjugate. Additionally, we observed that pLL35 from an evolved MG1655 had acquired an IS-element inserted intergenically between a hypothetical protein ORF and putative fimbrial subunit gene *flmA*.

Transcriptional responses to selection in MG1655. Given that MG1655 showed the strongest phenotypic responses to selection and contained a combination of strain-specific and shared mutational targets in evolved plasmid carriers, hereafter we focused our analyses on better understanding the evolutionary responses of this strain across treatments and replicate populations. We performed RNAseq on the ancestral genotype with or without pLL35 and on each of the evolved clones. In the ancestral MG1655, acquisition

of pLL35 caused a total of 17 chromosomal genes to be moderately differentially expressed (Log_2-fold change $\geq$1, FDR $\leq$0.05), with functions primarily related to metabolism (e.g., *dcuB*, *fumB*, *malK*, *gadX*, *hycD*; Fig. S5). Three genes in the L-threonine degradation operon *tdc* showed a common signature of upregulation. This modest transcriptional impact of the plasmid is consistent with the small but significant reduction in ancestral growth we observed in this strain, and more broadly is similar to the scale of transcriptional disruption caused by pLL35 in the other strains previously reported, albeit affecting largely different genes.

Next, we analyzed differential expression in the evolved clones relative to their ancestor to detect evolved transcriptional responses. A large fraction of significantly differentially transcribed genes (Log_2-fold change $\geq$1.5, FDR $\leq$0.05) were common to all treatments, that is occurring in both evolved plasmid-free and evolved plasmid-containing clones (n = 1450 genes; 59%), presumably representing general adaptation to the lab environment. In contrast, the remainder of differentially transcribed genes were only observed in evolved plasmid-carrying clones, potentially representing evolved transcriptional changes driven by the plasmid (Fig. 4). Among this subset, we focused on those significantly differentially transcribed in parallel in at least 3 replicate populations per treatment (n = 452) to identify those most likely to represent adaptive evolved responses. In general, most of these evolved changes led to downregulation (~80%, n = 363). Several functions exhibited plasmid-associated parallel transcriptional responses, including fimbrae (*fimCFGHI yehC*, *yqiL*), flagellar (*flgK*, *flgL*, *yfiR*), cellular adhesion (*ycbU*), DNA damage (*ybaZ*, *recG*, *uspC*), efflux (*envR*, *mdtB*, *ybhR*), LPS (*waaU*, *rfaBJ*, *rfaZ*), outer membrane (*dsbB*, *ompN*, *htrE*, *lpxA*, *qmcA*), and biofilm (*ycgZ*, *pgaBC*). In addition, several plasmid genes were significantly downregulated across both treatments. Many of these were hypothetical genes; however, several members of the *tra* operon were among the commonly downregulated genes. Indeed, the mean fold change expression-level of the *tra* genes was positively correlated with the relative rate of conjugation in evolved MG1655 plasmid-containing clones (R^2 = 0.468 P = 0.029; Fig. 5).

Three plasmid-containing evolved clones exhibited a transcriptional response distinct from the others. This response was characterized by strong upregulation of DNA-binding protein H-NS and strong downregulation of $bla_{CTX\text{-}M\text{-}15}$ and was associated with insertions of IS*1* or IS*3* between *hns* and *tdk*. Notably, the evolved clones with these IS-element insertions and consequently downregulated $bla_{CTX\text{-}M\text{-}15}$ expression tended to show reduced resistance to cefotaxime compared to the ancestral MG1655(pLL35) strain (Fig. 6). We identified 45 genes that were commonly and uniquely differentially expressed (Log_2 fold change $\geq$1.5, FDR $\leq$0.05) in clones containing insertions between *hns* and *tdk* (Fig. S6). All of these genes exhibited significant downregulation.

DISCUSSION

As plasmids transmit between bacterial lineages in microbial communities, they encounter diverse genomic backgrounds, wherein a given plasmid can have different fitness effects and cause varying levels and types of cellular disruption among strains (5, 6). The evolutionary response to plasmid acquisition in bacteria has been studied in a range of plasmid-host systems, providing evidence of evolutionary mechanisms that explain the widespread existence of plasmids in bacterial genomes (10, 12). However relatively few of these studies have compared evolutionary responses to gaining the same plasmid between genetically divergent strains, nor done so for a multidrug resistance plasmid in clinically relevant bacteria. In this study we examined the evolutionary response to plasmid acquisition after 700 generations by experimentally evolving genetically divergent *E. coli* lineages—including environmental, clinical and lab strains—with the MDR plasmid pLL35 in the presence and absence of antibiotic selection pressure.

We show that pLL35 acquisition imposed a small initial fitness cost in all the divergent *E. coli* strains we used. However, in only some of these strains did evolved clones show improved growth relative to their ancestor, notably strains MG1665 and F022, and such improvements were strongest in replicates evolved with cefotaxime. In addition, no

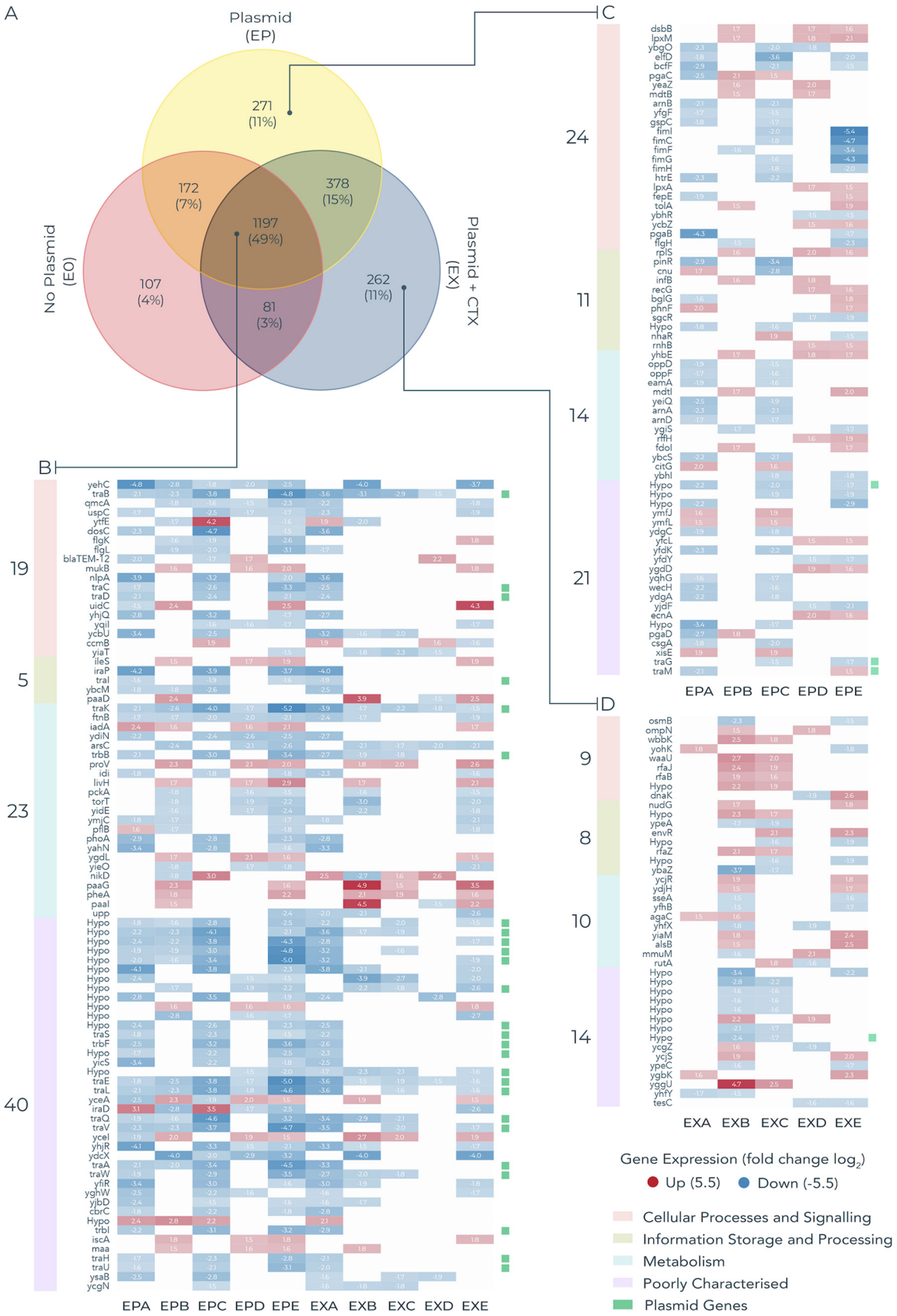

FIG 4 Transcriptional changes in *E. coli* MG1655 evolved clones. Genes that were significantly differentially expressed (Log_2 FC ≥1.5, FDR ≤0.05) in evolved clones relative to their ancestor. (A) Number of significantly differentially transcribed genes in each

(Continued on next page)

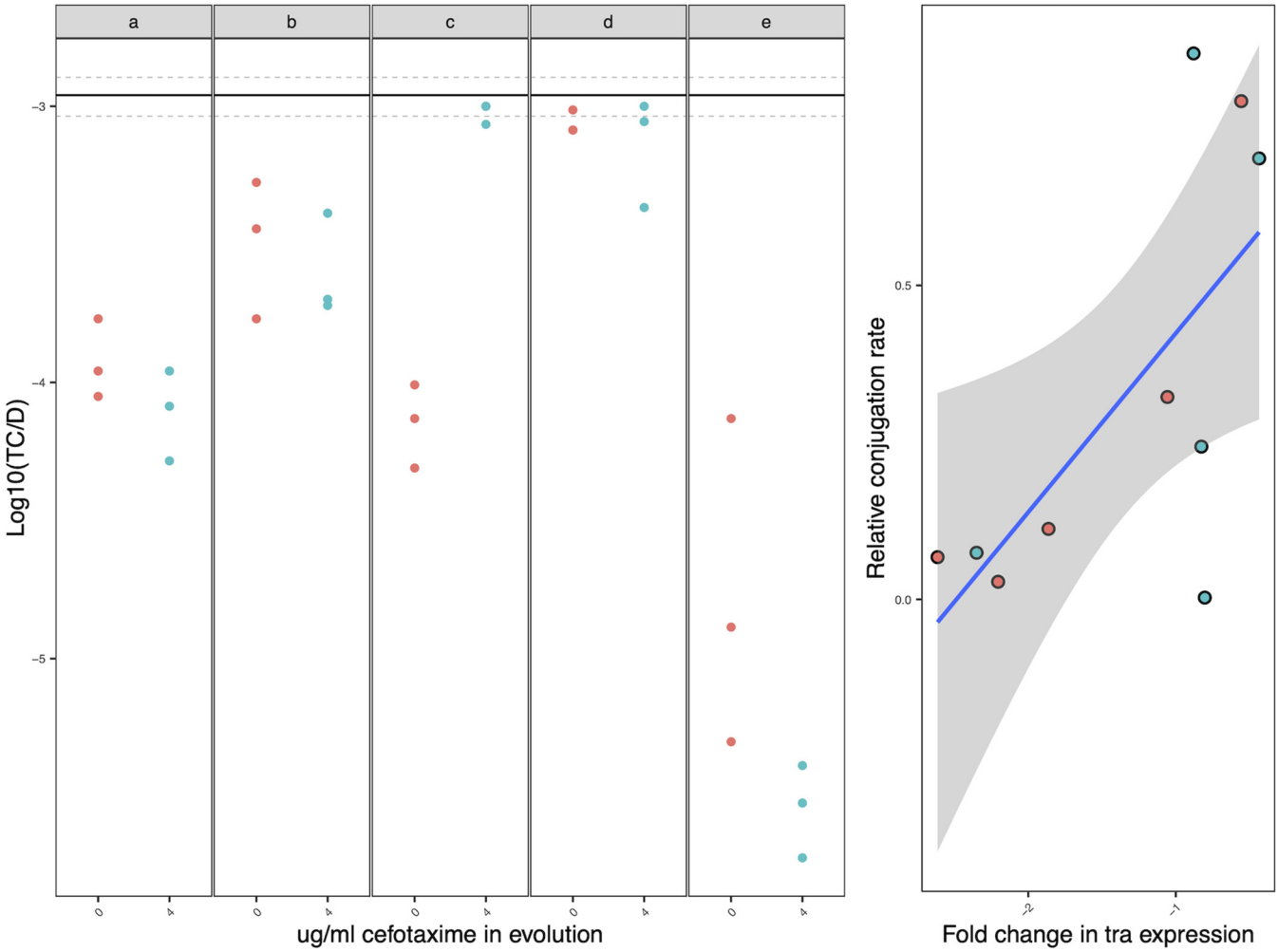

FIG 5 Conjugation rates and *tra* gene expression levels for evolved MG1655 plasmid carriers. Dots with no outline show conjugation rate estimates for evolved MG1655 clones facteted per replicate line evolved with (blue) or without (red) cefotaxime selection; data are shown for 3 technical replicates of the conjugation assay; the solid black line shows the ancestral conjugation rate and the dotted lines ± standard error. Dots with black outline show mean conjugation rates for evolved MG1655 clones relative to their ancestor plotted against the corresponding mean fold change in *tra* gene expression relative to their ancestor for the same evolved clone. The blue line is a linear regression and the gray ribbon indicates ± standard error.

consistent evolved changes to cefotaxime resistance were observed among strains, albeit with high divergence among replicates in some strains (e.g., MG1655). Nevertheless, by filtering for mutations that occurred exclusively in evolved plasmid carriers (i.e., those that did not occur in the corresponding plasmid-free control) and focusing on loci mutated in multiple replicate lines, we identified a range of chromosomal mutations putatively associated with adapting to plasmid carriage, some of which were common to multiple strains. These chromosomal mutations affected a wide range of operons but were enriched for metabolic and regulatory cellular functions. Plasmid mutations were less numerous and most commonly affected conjugation-related genes. On both the chromosome and the plasmid, we observed an important role for IS-mediated mutations in some strains, including insertion mutations impacting global regulatory systems (e.g., the DNA-binding protein H-NS) with effects on cefotaxime resistance unique to these evolved clones. A poten-

FIG 4 Legend (Continued)
evolution treatment. (B) Expression values of significantly differentially expressed genes that are common to both the EX and EP treatments. Only genes that are present in ≥3 evolved clones per treatment are displayed to prioritize genes that were under parallel selection. (C) Expression of genes that were uniquely differentially expressed in the EP treatment. (D) Expression of genes that are uniquely differentially expressed in the evolved EX treatment. Red cells indicate increased expression, blue cells indicate decreased expression relative to their ancestor. Plasmid genes are demarked with green squares. A number of plasmid genes are downregulated across several replicates of both treatment conditions, including a number of genes from the *tra* operon.

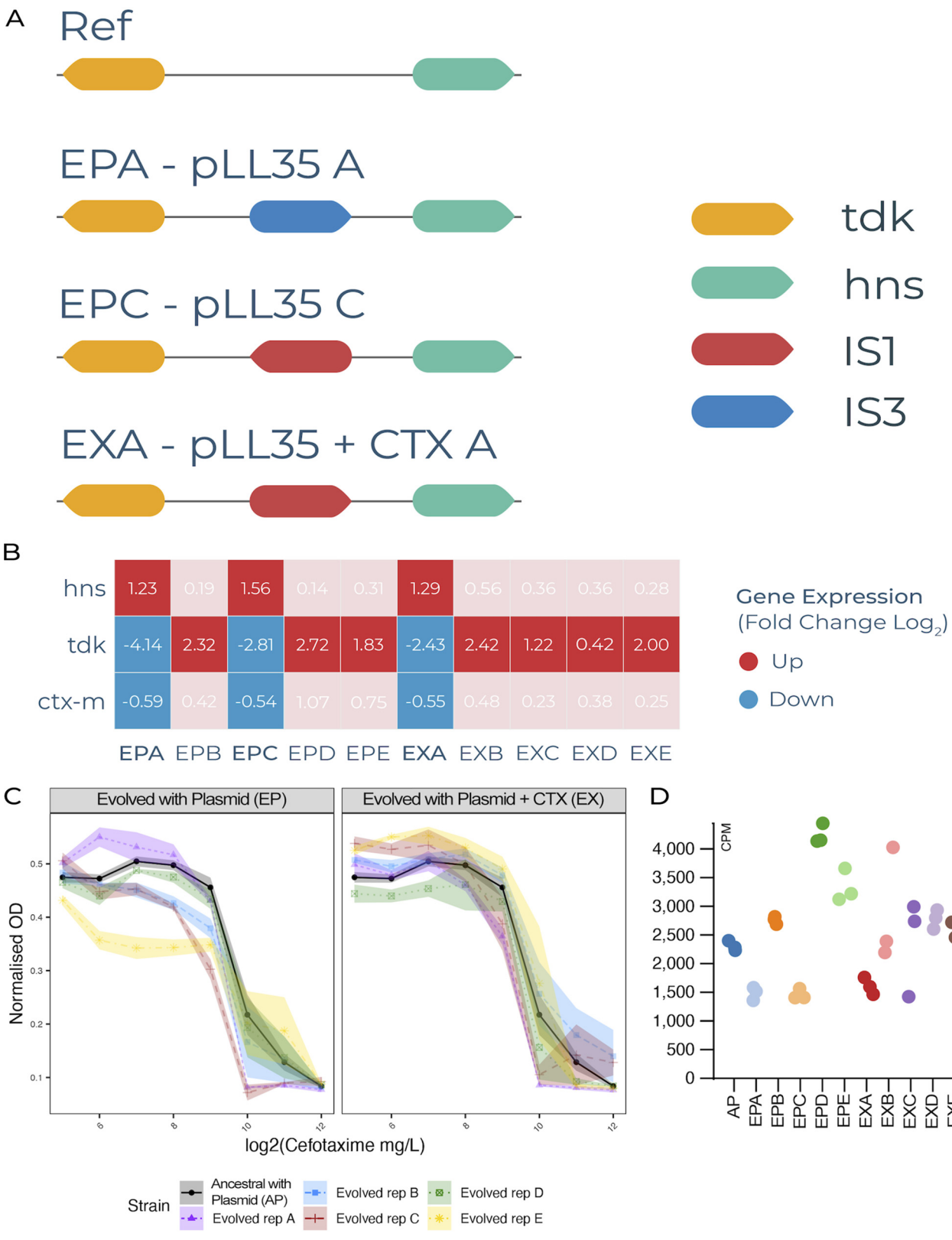

FIG 6 Transcriptional and resistance effects of IS-element insertions upstream of *hns*. Orientation and location of IS-element insertions between *hns* and *tdk* in 3 *E. coli* MG1655 plasmid-carrier evolved clones. (A) The reference configuration of the region, and the insertion position and orientation of IS-elements in evolved clones. (B) Differential expression of *hns*, *tdk* and $bla_{CTX\text{-}M\text{-}15}$ for all MG1655 plasmid-carrier evolved clones relative to their ancestor. Red cells indicate increased expression, blue cells indicate decreased expression relative to their ancestor. Darker shading indicates fold change Log_2 FC ≥1.0 relative to the clones lacking an IS-element insertion upstream of *hns*. (C) MIC curves against cefotaxime showing variation between the individual evolved and ancestral clones for the EP and EX treatments (different evolving lines denoted by colors; see visual key). (D) normalized transcript counts of $bla_{CTX\text{-}M\text{-}15}$ (counts per million) with the different evolving lines denoted by colors (see visual key).

tial cause of the mismatch between the small differences in relative growth versus strong evidence for adaptive mutations is that the relative growth assays we used are not a direct measure of relative fitness. Competition experiments wherein evolved strains are directly competed against their ancestor are the gold standard for quantifying fitness differences, having far greater sensitivity than optical density measurements of separately growing cultures as used here. Competition experiments rely, however, upon being able to introduce selectable markers into the ancestral competitor strains, but this is often not feasible for nonmodel clinical and environmental strains (as here), which are more challenging to genetically manipulate.

The majority of parallel chromosomal mutations associated with adapting to the plasmid occurred in genes involved in metabolism or its regulation. Several of these genes and operons include those that showed a transcriptional response in our previous RNAseq study of the immediate impact pLL35 acquisition in these strains, including *artP*, *nha*, and *put* (6). A notable finding of our previous study was a consistent low-level upregulation of genes involved in anaerobic metabolism caused by pLL35 across all the genetically divergent strains (6). Consistent with this conserved transcriptional response, here we observed parallel mutations in a wide range of genes associated with anaerobic metabolism, including anaerobic respiration (*norR*), fatty acid metabolism (*fad*) and fumarate metabolism (*dct*) in evolved plasmid carriers from multiple strains. This adds to a growing body of evidence suggesting that metabolism and the evolution of MDR *E. coli* are intrinsically linked. A pangenomic analysis of *E. coli* ST131 showed that this MDR clone was enriched in allelic variation in core anaerobic metabolism genes (23). Additionally, a study of diverse *E. coli* lineages grown under sub-inhibitory antibiotic selection pressure resulted in parallel adaptations in metabolism genes which potentiated resistance (24), and recent modeling studies have shown that evolution of AMR is strongly coupled to the evolution of major metabolic pathways (25). More generally, transcriptional and metabolomic studies suggest that a wide range of plasmids impact cellular metabolism in diverse bacterial taxa (26). For example, a previous study in *Pseudomonas aeruginosa* observed consistent metabolic responses to the acquisition of diverse antibiotic resistance plasmids (27). Why plasmids commonly alter cellular metabolism is currently unclear, but this may reflect a plasmid strategy designed to remodel bacterial metabolism in ways that are niche adaptive and boost plasmid vertical transmission (28). Our data suggest that, over the longer term, bacterial hosts may respond to plasmid metabolic manipulation through compensatory mutations in the affected metabolic pathways.

Although plasmid mutations were less commonly observed than those affecting chromosomal genes, plasmid mutations did arise in three of the *E. coli* strain backgrounds and almost all occurred in genes linked to conjugation. In one case, we observed the complete deletion of the conjugation operon, rendering the plasmid nonconjugative. Additionally, our RNAseq data showed that several evolved MG1655 plasmid carriers downregulated genes encoding components of the plasmid conjugation machinery and that reduced *tra* gene expression was associated with lower conjugation rates. The evolution of reduced conjugation is a common mechanism by which plasmids adapt to long-term association with a given bacterial host (16, 29, 30), and this is likely to reflect the burden of expressing the conjugative machinery for host cells and the absence of horizontal transmission fitness benefits for plasmids in populations without a supply of plasmid-free recipients cells (31). Notably, loss of conjugative ability was one of several possible routes of compensatory evolution for pOXA-48 plasmids in *E. coli* that have been observed to occur within patient infections (32).

Other resident mobile genetic elements (MGE), notably several insertion sequences, caused parallel mutations at a range of sites affecting both the chromosome and the plasmid in evolved plasmid carriers across multiple strains. We posit two nonmutually exclusive explanations for this pattern: First, MGE mobilization and expansion may be triggered by plasmid acquisition. Interactions between conjugative plasmids and resident MGEs have been observed for chromosomal transposons that respond and relocate to plasmids (13, 33), and have been implicated in the mobilization and spread of IS-associated ARGs by plasmids (34). Second, IS expansions may be a faster route to adaptation than point

mutations. This is consistent with previous *E. coli* experimental evolution studies, including the Long Term Evolution Experiment where an appreciable fraction of early beneficial mutations were caused by IS elements in nonmutator lineages (35), and coevolution of *E. coli* with MDR plasmids where adaptive mutations have been associated with IS element disruptions of chromosomal and plasmid genes (16–18, 20).

It is possible that the insertion of IS*1* and IS*3* into the region upstream of *hns* that occurred in parallel lines of MG1655 may have upregulated *hns*, consequently downregulating the $bla_{\text{CTX-M-15}}$ gene in pLL35, potentially causing the observed reduction in phenotypic resistance to cefotaxime. DNA-binding protein H-NS has been shown to play a key role in the controlled acquisition and integration of a number of virulence encoding MGEs such as *Salmonella* Pathogenicity Islands (36) and the Locus of Enterocyte Effacement in *E. coli* O157 (37), with DNA-binding protein H-NS silencing transcription of operons on those MGEs to minimize their impact on fitness when acquired. To our knowledge, a role for DNA-binding protein H-NS silencing during MDR plasmid acquisition has not previously been shown in *E. coli*. Our data suggest DNA-binding protein H-NS may offer a regulatory route by which *E. coli* adapts to MDR plasmids, potentially occurring here via the insertion of an IS element into the regulatory region of *hns* upregulating DNA-binding protein H-NS and in turn downregulating the newly acquired plasmid.

Using a comparative experimental evolution approach our study reveals a range of evolutionary pathways taken by genetically divergent *E. coli* lineages following acquisition of an MDR plasmid. In contrast to some studies where individual compensatory mutations ameliorated plasmid fitness costs, we did not see evidence for a major genetic conflict between chromosome and plasmid that could be fixed by single point mutations (cf. (13)). Rather we observed a more complex evolutionary process targeting a wide range of functions, including cellular metabolic pathways impacted by plasmid carriage, plasmid conjugation, and global regulatory systems controlling expression of foreign DNA. Our results highlight the importance of interactions between incoming plasmids and MGEs already resident in the cell, both in terms of IS elements relocating to plasmids and their expansion causing parallel mutations, an emerging theme in plasmid-host evolution (16–18, 20). The key challenge for future work will be to understand how these evolutionary processes translate from the lab into more infection-relevant conditions to better understand the success of specific plasmid-host combinations in clinical settings.

MATERIALS AND METHODS

Bacterial strains and plasmids. Five genetically diverse *E. coli* strains were used as hosts for the 106 kb FII(K)-9 multidrug resistance plasmid pLL35 (6). Specifically, these included clinical isolates (F022, sequence type ST-131 A; F054, sequence type ST-131 B; F104, sequence type ST-131 C), an environmental isolate (ELU39, sequence type ST-1122), and the lab strain MG1655. Some of these strains carry other plasmids (described in [6]). Five independent colonies were isolated per strain for use as ancestral genotypes in the evolution experiments and stored cryogenically for subsequent use (plasmid-free ancestrals). For use in plasmid-containing treatments, pLL35 was conjugated into each of these ancestral genotypes from its natural host (*Klebsiella pneumoniae*), generating five independent transconjugants per strain (ancestrals). Specifically, each single colony was inoculated into 5 mL of nutrient broth (NB; Oxoid, United Kingdom) and incubated at 37°C for 2 h with shaking (180 rpm). *K. pneumoniae* donor and *E. coli* recipient cultures were mixed at a ratio of 1:3, and 50 μL was used to inoculate 6 mL of brain heart infusion (BHI) broth. These were then incubated as static cultures at 37°C for 24 h. The conjugation mixture was plated onto 4 μg/mL of cefotaxime UTI Chromagar (Sigma-Aldrich, United Kingdom) and incubated at 37°C overnight. Pink *E. coli* transconjugant colonies were then subcultured onto UTI Chromagar with 4 μg/mL of cefotaxime and stored cryogenically for subsequent use.

Selection experiment. We isolated five independent plasmid-free and plasmid-carrying ancestral clones per strain. Each of these was re-streaked onto a nutrient agar plate, incubated at 37°C for 24 h, and a single colony from each plate was then used to inoculate an overnight liquid culture in 6 mL of NB. To establish replicate populations for the selection experiment, 60 μL of the respective overnight culture was used per treatment. Plasmid-carriers were propagated by 1% daily serial transfer in 6 mL NB liquid cultures under two treatments: Specifically, replicate plasmid-carrier populations were propagated either with (evolved with plasmid plus cefotaxime treatment; EX) or without (evolved with plasmid treatment; EP) 4 μg/mL of cefotaxime supplementation. In addition, plasmid-free controls were propagated under equivalent conditions without cefotaxime supplementation (control treatment; EC). This experimental design resulted in 75 independently evolving lines that were maintained for 84 days. For all treatments, every 14 days serial dilutions of each population were plated out onto nutrient agar plates $\pm$ 4 μg/mL of cefotaxime to quantify the total population density and the density of cefotaxime resistance. For the EX and EP treatments, every 28 days 24 colonies

from the cefotaxime supplemented agar plates were picked and tested for the presence of the plasmid backbone and the $bla_{CTX\text{-}M\text{-}15}$ gene by PCR using a previously published protocol (6).

Growth kinetics assays. Growth kinetics were obtained for each plasmid-free and plasmid-carrying ancestral clone and for a single colony randomly chosen from each evolving line at the endpoint of the selection experiment (i.e., day 84). Triplicate cultures of each clone were grown in 200 μL NB per well in 96-well plates incubated at 37°C for 24 h. Optical density (OD) at 600 nm was recorded every 30 min for 24 h using an automated absorbance plate reader (Tecan Spark 10). Prior to each reading, plates were shaken for 5s at 180 rpm orbital shaking with a movement amplitude of 3 mm. A humidity cassette was used to minimize evaporation. From the resulting growth curves were calculated: maximum absorbance reached in 24 h (OD600), lag period calculated as *x* axis intercept (time, hours) of a tangent to the growth curve at the point of maximum growth rate, maximum growth rate, and integral of growth curve as area under the curve. To assess the effect of plasmid acquisition in the ancestral strains, relative growth parameters were calculated by dividing the corresponding parameter of the plasmid-carrying ancestor by the corresponding parameter of the plasmid-free ancestor. To assess the effect of evolution on growth parameters, relative growth parameters were calculated by dividing the growth parameters of evolved strains by the corresponding parameter of their ancestor (i.e., for plasmid-free evolved clones this would be the relevant plasmid-free ancestral strain, whereas for plasmid-carrying evolved clones this would be the relevant plasmid-containing ancestral strain).

Cefotaxime resistance assays. MIC assays for each plasmid-free and plasmid-carrying ancestral clone and for a single colony randomly chosen from each evolving line at the endpoint of the selection experiment (i.e., day 84) were conducted according to the CLSI guidelines (38), using nutrient broth and cefotaxime. Shaking (180 rpm) overnight cultures in 6 mL nutrient broth were established from independent colonies previously grown on agar plates. The following day, 0.5 McFarland cell suspensions were prepared and further diluted 1/500 to inoculate 200 μL of nutrient broth in 96-well plates. The final cefotaxime concentrations tested were 2-fold increases from 64 to 8192 μg/mL, and the final volume per well was 200 μL (100 μL bacterial inoculum plus 100 μL antibiotic solution). The OD_{600} was recorded after 24 h of static incubation at 37°C and normalized by subtracting the OD_{600} of a blank well. As working with positive OD_{600} values facilitates further data analysis and interpretation, we linearly transformed OD_{600} estimates by adding 0.0819 to all data. For each strain and plasmid combination, the relative growth at each antibiotic concentration was obtained by dividing OD_{600}values in the presence of antibiotic by the OD_{600} of the corresponding parental strain grown in the absence of antibiotic. The relative growth values were used to calculate the area under the curve (AUC) with the auc function from the R package flux (flux_0.3-0). Statistical analyses were performed on Box Cox transformed data to fulfill ANOVA assumptions.

Plasmid transfer assays. pLL35 transfer frequencies were assessed by mating ancestral or evolved MG1655 containing pLL35 with a nalidixic acid-resistant derivative of a GFP-labeled plasmid-free MG1655 (17). 100 μL each of MG1655(pLL35) donor and MG1655::GFP recipient were mixed by spreading on a Mueller-Hinton agar plate and incubated at 37°C for 18 h. The resulting bacterial lawn was harvested in sterile phosphate-buffered saline and serially diluted in a 10-fold series. Dilutions were plated on Mueller-Hinton agar containing 4 μg/mL cefotaxime to select for MG1655(pLL35), and Mueller-Hinton agar containing 4 μg/mL cefotaxime and 25 μg/mL nalidixic acid to select for pLL35-containing MG1655::GFP transconjugants. Transfer frequencies were determined as the number of transconjugants per donor.

Statistical analysis. RStudio was used to perform statistical analysis. R packages used were lme4 (version [v] 1.1-26); ART (v. 1.0); car (v. 3.0-8); MASS (v. 7.3-53); nlme (v. 3.1-148); rcompanion (2.4.1); flux (v. 0.3-0). The bacterial densities from the evolution experiment were analyzed in a linear mixed-effects model (LMM). Strain, treatment and the number of serial transfers were introduced in the model as fixed effects, whereas population was used as a random effect to account for repeated measures. Data required a Box-Cox transformation to meet model assumptions. We reduced the model by performing likelihood ratio tests on nested models. The impact of strain and evolution treatment on growth kinetic parameters, including the area under the curve, the maximum growth rate, the maximum optical density, and the lag time of the evolved strains relative to their corresponding ancestral, were assessed. These relative growth parameters were analyzed using ANOVA, art ANOVA, or Scheirer-Ray-Hare test depending on the data characteristic and if the assumptions of the tests were met. A Box-Cox transformation was applied when required. To analyze change in MIC following evolution, we performed an ART ANOVA of the area under the MIC curve of evolved clones relative to their ancestor fitting strain and treatment. Further statistical analyses were performed for each strain individually.

Genomics and bioinformatics. We obtained whole-genome sequences for one randomly chosen colony per evolving line taken from the endpoint of the selection experiment (i.e., day 84) using both Illumina and Oxford Nanopore Technology platforms. Sequencing data is available under BioProject accession number PRJNA848631, and a list of isolate accession numbers is provided in Table S3. Ancestral WGS data are available under Bioproject Accession number PRJNA667580, and are described in (6).

The long reads were processed with FiltLong (V 0.2.0) to remove short or low quality reads (<1000 bp, <Q6), and chimeric reads were removed using Unicycler's (V 0.4.7) scrub module. The distributions of qualities and lengths of reads were assessed and visualized using NanoPlot (V 1.20.0). Where there was an abundance of reads, the data was subsampled to 100X coverage to reduce computational cost. Assemblies were constructed using Unicycler (V 0.4.7) using normal bridging mode. In a minor number of instances, small repetitive elements were not fully resolved, to address this, we also assembled our isolates with Trycycler (V 0.4.1), which uses iterative subsampling and assembly of differential read sets and obtains a consensus. These assemblies were then polished using Racon (V1.4.10), Medaka (V 1.0.3), and Pilon (V 1.23) (implemented through unicycler_polish), using both long and short reads respectively. The genomes were annotated using Prokka (V 1.14.6). Assemblies were screened for insertion sequences using isescan (V 1.7.2), which identified a number of novel IS movements. These movements were further investigated using Artemis Comparison Tool, and

adjacent sections of sequence were identified using both the annotation files and BLAST against the nonredundant bacterial protein database.

Variants were called against fully resolved and annotated assemblies using Breseq (V 0.35.4), using additional flags to ensure a minimum variant base depth of 10, quality of 20, and allele frequency of 0.9. We also assessed structural variation using Sniffles (V 1.0.12) and Assemblytics (commit #58fb525). Any deletions were verified by mapping the Illumina read sets against the assembly using Bowtie2 (V 4.8.2) and identifying regions of missing coverage. For our final list of variants, we masked any variants that occurred in the evolved no plasmid (EC) lines, as these represent basal adaptation to the media and laboratory conditions. Protein annotations in which a variant was detected were confirmed using BLAST, and where possible hypothetical proteins were assigned putative functions or families. Data visualization was conducted using R (V 3.4.3) and ggplot (V 3.3.3), and GraphPad Prism (V 7).

Transcriptomics and bioinfomatics. We obtained transcriptomes for MG1655 plasmid-free and plasmid-carrying ancestral clones and for each sequenced MG1655 evolved clone taken from the endpoint of the selection experiment (i.e., day 84). Triplicate shaken cultures were grown at 37°C to an OD600 of 0.6 in 10 mL of nutrient broth and centrifuged. Residual media was discarded, and the cell pellet was snap-frozen. Samples were shipped to GeneWiz, who performed the RNA extractions, and sequenced the purified RNA on an Illumina NovaSeq configured to 2 × 150 bp cycles.

Kallisto (V 0.46.0) was used to quantify differential gene expression, with the high-quality hybrid *de novo* assemblies of the relevant ancestral strain was used as a reference. Input files were prepared using Prokka (V 1.13.3) for annotation, genbank_to_kallisto.py (https://github.com/AnnaSyme/genbank_to_kallisto.py) to convert the annotation files for use with Kallisto, and GNU-Parallel (V 20180922) for job parallelization. Differential gene expression was analyzed using Voom/Limma in Degust (V 3.20), with further processing of the resulting differential counts in R (V 3.5.3). Functional categories (COG, GO-terms) were assigned to genes using eggnog-mapper (V 2).

Data availability. All experimental data sets are provided in the supplemental material of this article. Sequencing data is available under BioProject accession number PRJNA848631, and a list of isolate accession numbers is provided in Table S3. Ancestral WGS data are available under Bioproject Accession number PRJNA667580, and are described in (6).

SUPPLEMENTAL MATERIAL

Supplemental material is available online only.

DATA SET S1, XLS file, 1 MB.
FIG S1, JPG file, 0.5 MB.
FIG S2, JPG file, 0.4 MB.
FIG S3, JPG file, 0.3 MB.
FIG S4, JPG file, 1 MB.
FIG S5, JPG file, 0.1 MB.
FIG S6, JPG file, 0.6 MB.
TABLE S1, XLSX file, 0.01 MB.
TABLE S2, XLSX file, 0.01 MB.
TABLE S3, DOCX file, 0.02 MB.

ACKNOWLEDGMENTS

This work was funded by Biotechnology and Biological Sciences Research Council grants BB/R006261/1, BB/R006253/1 and BB/R006253/2 and supported by the NIHR Manchester Biomedical Research Centre.

REFERENCES

1. Mathers AJ, Peirano G, Pitout JDD. 2015. The role of epidemic resistance plasmids and international high-risk clones in the spread of multidrug-resistant Enterobacteriaceae. Clin Microbiol Rev 28:565–591. https://doi.org/10.1128/CMR.00116-14.
2. Dunn SJ, Connor C, McNally A. 2019. The evolution and transmission of multi-drug resistant Escherichia coil and Klebsiella pneumoniae: the complexity of clones and plasmids. Curr Opin Microbiol 51:51–56. https://doi.org/10.1016/j.mib.2019.06.004.
3. Cantón R, Coque TM. 2006. The CTX-M beta-lactamase pandemic. Curr Opin Microbiol 9:466–475. https://doi.org/10.1016/j.mib.2006.08.011.
4. Lartigue M-F, Poirel L, Aubert D, Nordmann P. 2006. In vitro analysis of ISEcp1B-mediated mobilization of naturally occurring beta-lactamase gene blaCTX-M of Kluyvera ascorbata. Antimicrob Agents Chemother 50:1282–1286. https://doi.org/10.1128/AAC.50.4.1282-1286.2006.
5. Alonso-del Valle A, Leon-Sampedro R, Rodriguez-Beltran J, DelaFuente J, Hernandez-Garcia M, Ruiz-Garbajosa P, Canton R, Pena-Miller R, San MA. 2021. Variability of plasmid fitness effects contributes to plasmid persistence in bacterial communities. Nat Commun 12:2653. https://doi.org/10.1038/s41467-021-22849-y.
6. Dunn S, Carrilero L, Brockhurst M, McNally A. 2021. Limited and strain-specific transcriptional and growth responses to acquisition of a multidrug resistance plasmid in genetically diverse Escherichia coli lineages. mSystems 6:e00083-21. https://doi.org/10.1128/mSystems.00083-21.
7. Gama JA, Kloos J, Johnsen PJ, Samuelsen O. 2020. Host dependent maintenance of a bla(NDM-1)-encoding plasmid in clinical Escherichia coli isolates. Sci Rep 10:9332. https://doi.org/10.1038/s41598-020-66239-8.
8. Bergstrom C, Lipsitch M, Levin B. 2000. Natural selection, infectious transfer and the existence conditions for bacterial plasmids. Genetics 155:1505–1519. https://doi.org/10.1093/genetics/155.4.1505.

9. Harrison E, Brockhurst MA. 2012. Plasmid-mediated horizontal gene transfer is a coevolutionary process. Trends Microbiol 20:262–267. https://doi.org/10.1016/j.tim.2012.04.003.
10. San Millan A. 2018. Evolution of plasmid-mediated antibiotic resistance in the clinical context. Trends Microbiol 26:978–985. https://doi.org/10.1016/j.tim.2018.06.007.
11. San Millan A, Maclean RC. 2017. Fitness costs of plasmids: a limit to plasmid transmission. Microbiol Spectr 5. https://doi.org/10.1128/microbiolspec.MTBP-0016-2017.
12. Brockhurst MA, Harrison E. 2022. Ecological and evolutionary solutions to the plasmid paradox. Trends Microbiol 30:534–543. https://doi.org/10.1016/j.tim.2021.11.001.
13. Hall JPJ, Wright RCT, Harrison E, Muddiman KJ, Wood AJ, Paterson S, Brockhurst MA. 2021. Plasmid fitness costs are caused by specific genetic conflicts enabling resolution by compensatory mutation. PLoS Biol 19:e3001225. https://doi.org/10.1371/journal.pbio.3001225.
14. Loftie-Eaton W, Bashford K, Quinn H, Dong K, Millstein J, Hunter S, Thomason MK, Merrikh H, Ponciano JM, Top EM. 2017. Compensatory mutations improve general permissiveness to antibiotic resistance plasmids. Nat Ecol Evol 1:1354–1363. https://doi.org/10.1038/s41559-017-0243-2.
15. Millan AS, Toll-Riera M, Qi Q, MacLean RC. 2015. Interactions between horizontally acquired genes create a fitness cost in Pseudomonas aeruginosa. Nat Commun 6:6845. https://doi.org/10.1038/ncomms7845.
16. Porse A, Schønning K, Munck C, Sommer MOA. 2016. Survival and evolution of a large multidrug resistance plasmid in new clinical bacterial hosts. Mol Biol Evol 33:2860–2873. https://doi.org/10.1093/molbev/msw163.
17. Bottery MJ, Wood AJ, Brockhurst MA. 2017. Adaptive modulation of antibiotic resistance through intragenomic coevolution. Nat Ecol Evol 1:1364–1369. https://doi.org/10.1038/s41559-017-0242-3.
18. Bottery MJ, Wood AJ, Brockhurst MA. 2019. Temporal dynamics of bacteria-plasmid coevolution under antibiotic selection. Isme J 13:559–562. https://doi.org/10.1038/s41396-018-0276-9.
19. Jordt H, Stalder T, Kosterlitz O, Ponciano JM, Top EM, Kerr B. 2020. Coevolution of host-plasmid pairs facilitates the emergence of novel multidrug resistance. Nat Ecol Evol 4:863–869. https://doi.org/10.1038/s41559-020-1170-1.
20. Benz F, Hall AR. 2022. Host-specific plasmid evolution explains the variable spread of clinical antibiotic-resistance plasmids. bioRxiv. https://doi.org/10.1101/2022.07.06.498992.
21. Carattoli A. 2009. Resistance Plasmid Families in *Enterobacteriaceae*. Antimicrob Agents Chemother 53:2227–2238. https://doi.org/10.1128/AAC.01707-08.
22. Matlock W, Chau KK, AbuOun M, Stubberfield E, Barker L, Kavanagh J, Pickford H, Gilson D, Smith RP, Gweon HS, Hoosdally SJ, Swann J, Sebra R, Bailey MJ, Peto TEA, Crook DW, Anjum MF, Read DS, Walker AS, Stoesser N, Shaw LP, AbuOun M, Anjum MF, Bailey MJ, Brett H, Bowes MJ, Chau KK, Crook DW, de Maio N, Duggett N, Wilson DJ, Gilson D, Gweon HS, Hubbard A, Hoosdally SJ, Matlock W, Kavanagh J, Jones H, Peto TEA, Read DS, Sebra R, Shaw LP, Sheppard AE, Smith RP, Stubberfield E, Stoesser N, Swann J, Walker AS, Woodford N, REHAB consortium. 2021. Genomic network analysis of environmental and livestock F-type plasmid populations. Isme J 15:2322–2335. https://doi.org/10.1038/s41396-021-00926-w.
23. McNally A, Kallonen T, Connor C, Abudahab K, Aanensen DM, Horner C, Peacock SJ, Parkhill J, Croucher NJ, Corander J. 2019. Diversification of colonization factors in a multidrug-resistant Escherichia coli lineage evolving under negative frequency-dependent selection. mBio 10:e00644-19. https://doi.org/10.1128/mBio.00644-19.
24. Lopatkin AJ, Bening SC, Manson AL, Stokes JM, Kohanski MA, Badran AH, Earl AM, Cheney NJ, Yang JH, Collins JJ. 2021. Clinically relevant mutations in core metabolic genes confer antibiotic resistance. Science 371:eaba0862. https://doi.org/10.1126/science.aba0862.
25. Pinheiro F, Warsi O, Andersson DI, Lässig M. 2021. Metabolic fitness landscapes predict the evolution of antibiotic resistance. Nat Ecol Evol 5:677–687. https://doi.org/10.1038/s41559-021-01397-0.
26. Vial L, Hommais F. 2020. Plasmid-chromosome cross-talks. Environ Microbiol 22:540–556. https://doi.org/10.1111/1462-2920.14880.
27. San Millan A, Toll-Riera M, Qi Q, Betts A, Hopkinson RJ, McCullagh J, MacLean RC. 2018. Integrative analysis of fitness and metabolic effects of plasmids in Pseudomonas aeruginosa PAO1. Isme J 12:3014–3024. https://doi.org/10.1038/s41396-018-0224-8.
28. Billane K, Harrison E, Cameron D, Brockhurst MA. 2022. Why do plasmids manipulate the expression of bacterial phenotypes? Philosophical Transactions B 377:20200461. https://doi.org/10.1098/rstb.2020.0461.
29. Dahlberg C, Chao L. 2003. Amelioration of the cost of conjugative plasmid carriage in Escherichia coli K12. Genetics 165:1641–1649. https://doi.org/10.1093/genetics/165.4.1641.
30. Turner PE, Williams ESCP, Okeke C, Cooper VS, Duffy S, Wertz JE. 2014. Antibiotic resistance correlates with transmission in plasmid evolution. Evolution 68:3368–3380. https://doi.org/10.1111/evo.12537.
31. Hall JPJ, Brockhurst MA, Dytham C, Harrison E. 2017. The evolution of plasmid stability: Are infectious transmission and compensatory evolution competing evolutionary trajectories? Plasmid 91:90–95. https://doi.org/10.1016/j.plasmid.2017.04.003.
32. DelaFuente J, Toribio-Celestino L, Santos-Lopez A, et al. 2022. Within-patient evolution of plasmid-mediated antimicrobial resistance. Nat Ecol Evol 6:1980–1991. https://doi.org/10.1038/s41559-022-01908-7.
33. Hall JPJ, Williams D, Paterson S, Harrison E, Brockhurst MA. 2017. Positive selection inhibits gene mobilization and transfer in soil bacterial communities. Nat Ecol Evol 1:1348–1353. https://doi.org/10.1038/s41559-017-0250-3.
34. Che Y, Yang Y, Xu X, Břinda K, Polz MF, Hanage WP, Zhang T. 2021. Conjugative plasmids interact with insertion sequences to shape the horizontal transfer of antimicrobial resistance genes. Proc Natl Acad Sci U S A 118:e2008731118. https://doi.org/10.1073/pnas.2008731118.
35. Consuegra J, Gaffé J, Lenski RE, Hindré T, Barrick JE, Tenaillon O, Schneider D. 2021. Insertion-sequence-mediated mutations both promote and constrain evolvability during a long-term experiment with bacteria. Nat Commun 12:980. https://doi.org/10.1038/s41467-021-21210-7.
36. Ali SS, Soo J, Rao C, Leung AS, Ngai DH-M, Ensminger AW, Navarre WW. 2014. Silencing by H-NS potentiated the evolution of Salmonella. PLoS Pathog 10:e1004500. https://doi.org/10.1371/journal.ppat.1004500.
37. Sperandio V, Mellies JL, Nguyen W, Shin S, Kaper JB. 1999. Quorum sensing controls expression of the type III secretion gene transcription and protein secretion in enterohemorrhagic and enteropathogenic Escherichia coli. Proc Natl Acad Sci U S A 96:15196–15201. https://doi.org/10.1073/pnas.96.26.15196.
38. Wikler M, Cockerill F, Craig W. 2006. Method for dilution antimicrobial test for bacteria that grow aerobically; approved standard. Clinical and Laboratory Standards Institute, Wayne, PA.